Al-Shakarchi and Abd-Almajied Iraqi Journal of Science, 2022, Vol. 63, No. 10, pp: 4576-4586
DOI: 10.24996/ijs.2022.63.10.39

ISSN: 0067-2904

Response of The Ionospheric *E*- Region Critical Frequency and Virtual Height to the Solar Cycle 22 over Baghdad

Duraid A. Al-Shakarchi [1]*, Mohammed I Abd-Almajied [2]
[1] Department of Astronomy & Space, University of Baghdad, Baghdad, Iraq
[2] Remote sensing and GIS Department, University of Baghdad, Baghdad, Iraq

Received: 2/2/2022 Accepted: 29/5/2022 Published: 30/10/2022

Abstract
The aim of this study is to investigate the response of the Ionospheric *E*- region critical frequency f_oE and virtual height $h'E$ parameters to the solar cycle 22 over Baghdad city (latitude 33.3˚N, longitude 44.4˚E). Both parameters display a high relationship with the sunspot relative number within the ascending and descending phases of the solar cycle. The *E* - region response to the solar activity is obvious around noon, sunrise and sunset times. Moreover, the gap between local mid-afternoon, dawn and sunset values expands as solar activity rises. In the declining phase, there is an aspect that results in a peak of disturbance. This portion may have linked to coronal holes and resulted in high disturbance peak during 1992-1994. The impact of this portion is obvious in raising the values of f_oE, especially in 1993.

Keywords: Ionosphere, solar cycle, *E*- region, HF radio wave propagation, critical frequency, virtual height

استجابة التردد الحرج والارتفاع الظاهري لمنطقة *E* – الأيونوسفيرية للدورة الشمسية 22 فوق بغداد

دريد عبدالسلام الشكرجي [1]* , محمد اسماعيل عبدالمجيد [2]
[1] قسم الفلك والفضاء, كلية العلوم, جامعة بغداد, بغداد, العراق
[2] قسم التحسس النائي ونظم المعلومات الجغرافية, كلية العلوم, جامعة بغداد, بغداد, العراق

الخلاصة
الهدف من الدراسة هو التحقق في استجابة معاملات التردد الحرج f_oE والارتفاع الظاهري $h'E$ للمنطقة الأيونوسفيرية *E* للدورة الشمسية 22 فوق مدينة بغداد (خط العرض 33.3 درجة شمالاً ، وخط الطول 44.4 درجة شرقاً). أظهر كلا المعاملين علاقة كبيرة مع العدد النسبي للبقع الشمسية في مرحلتي الصعود والهبوط من الدورة الشمسية. استجابة المنطقة– *E* للنشاط الشمسي كانت واضحة في أوقات الظهيرة , شروق الشمس وغروبها. علاوة على ذلك ، اتساع الفجوة بين القيم المحلية لمنتصف النهار والفجر وغروب الشمس مع ارتفاع النشاط الشمسي. في مرحلة الانحدار من الدورة الشمسية ، هناك جانب يشهد ذروة في الاضطراب . هذا الجزء قد يكون مرتبطًا بالثقوب الإكليلية وأدى إلى ذروة اضطراب عالية خلال الفترة 1992–1994. إن تأثير هذا الجزء واضح في رفع قيم *foE* ، خاصة في العام 1993.

*Email: duraid.mohammed@sc.uobaghdad.edu.iq

1. Introduction

The region of Ionosphere is part of the upper atmosphere, located roughly between about 60 to 1000 km of height, in which free electrons and ions are sufficiently high to influence the high frequency radio wave propagation. At mid latitudes, the Ionosphere is basically produced by the solar electromagnetic radiations including extreme ultraviolet (EUV), and X-ray. Both radiations have an impact on a different layer of the Ionosphere [1, 2].

The theoretical and modern experiments divide the ionosphere into three regions: *D*, *E*, and *F*. The upper ionosphere *F*- region (between 140 and 600 km in altitude) has the greatest concentration of free electrons and splits into *F1* and *F2*, while the D layer (between 50 and 90 km) vanishes completely at night. The *F*- region is distinguished by the transfer of charged particles in plasma by some complex physical mechanisms, such as thermospheric winds and ambipolar diffusion. However, the mid ionosphere layer (*E*- region of altitude 90–140 km) marks the limit of ionization-recombination together with the dynamic and thermal operations. The heights of the ionospheric regions vary with solar zenith angle, time of day, seasons, and short and long term solar activity [3].

For mid latitude region, several studies have discussed the relation between solar activity and *E* region parameters, such as critical frequencies, virtual heights, and total electron contents. In Iraq, the earlier studies of *E*- region were in the early eighties of the last century. R. A. Ishak studied the statistical variations of the general characteristics of ionospheric layers during 1983, depending on the observations of Ionosonde which were installed in Al-Battani observatory, north of Baghdad [4]. These variations were discussed and compared with the variations of the Sunspot number(R) and the solar zenith angle (χ). Using the same ionospheric station measurements, K. Mouala and B. A. Rahman studied the daily and seasonal behavior of *E*- region over Baghdad during 1983 [5]. They found that *E*- region height over Baghdad extended from about 90-160 km. The maximum electron density located at an altitude of 114 km, and the maximum values of seasonal electron density occurred during summer. *E*- layer over Baghdad that appears at summer nights during disturbed geomagnetic conditions is associated with low critical frequencies and height. In two other studies in Iraq, Al-Shakarchi D. A. and D. A. Mohammed *et al*. relied on the data of Al-Battani observatory Ionosonde to investigate the impact of solar cycle 22 on the two upper regions of the ionosphere, *F1* and *F2* [6, 7]. Both found a high relationship between the solar cycle and the f_oF2 and f_oF1, respectively. Recently, two studies have investigated *E*-region critical frequency and electron density parameters over Iraq using the International Reference Ionosphere (IRI-2016) model. Khalid A. Hadi and A. A. Hamied investigated the impact of solar cycles 22, 23, and 24 on the annual critical frequencies of *E, F1*, and *F2* in Iraq [8]. Annual fluctuations in f_oE for the years 1989, 2001, and 2014 found that the values were nearly consistent, with occasional variations in the southern parts. In addition, there are slight differences in the variations for the years (1986, 1996, and 2008). On the other hand, Asma'a A. Hamied and Khalid A. Hadi studied the annual behavior of f_oE and electron density(N_e) for the solar cycle maximum years (1989, 2001 and 2014) and the minimum years (1986, 1996 and 2008) [9]. The variations for the tested years revealed small variances between them, with larger values during solar cycle maximum years and lower values during solar cycle minimum years.

In this study, the variations of two important *E*- region parameters (f_oE & *h'E*) have been discussed due to the solar cycle 22 over Baghdad, which located on the mid- latitude region (latitude= 33.3° N). Solar cycle 22 duration was from September 1986 to May 1996.

2. The Ionospheric *E*-layer

E region starts from the altitude of about 90- 140 km. Sometimes it contains a sporadic *E* layer (E_s), which is considered to be an independent phenomenon from the normal *E*- region.

Ionization at *E*- region is caused mainly by *X*- rays in the (1-17)nm and EUV in the (80-102.6)nm (L-Beta), producing ionized particles with a domination of NO^+ and O_2^+. In addition, *E*- region contains electrons with concentration less than 4 MHz. This value drops rapidly after sunset to a very low concentration.
The *E* layer exhibits the Chapman model behavior with daily maximum at local noon, seasonal maximum in summer, and solar cycle dependence. The basic Chapman theory of ionized layer formation begins with monochromatic radiation acting on a plane atmosphere with a single ionnizable gas with a constant scale height [3, 10].

3. Critical Frequency and Virtual Height

The process and instrumentation used to calculate the ionosphere's electron density as a function of altitude are based on the principle that when an electromagnetic wave vertically penetrates ionospheric plasma, it reflects at the level where the refractive index (*n)* becomes zero. The refractive index is defined as the ratio of the sine of the angle of incidence *Øi* to the sine of the angle of refraction *Ør* for a given pair of media [11]:

$$n = \sin Øi / \sin Ør = \sqrt{1-(81N / f^2)} \quad (1)$$

where *f* is the frequency of the radio wave in hertz, *N* is the number of free electrons per cubic meter (el/m^3). According to the magneto-ionic theory of the reflection of radio waves from the ionosphere, *n* is dependent on the plasma frequency f_N:

$$n^2 = 1 - (f_N / f)^2 \quad (2)$$

Where f_N and *f* are plasma and incident frequencies respectively.

$$f_N = \sqrt{Nq^2/(4\pi^2\varepsilon_\circ m)} \quad (3)$$

Where *N* is electron density, *q* is charge of electron, $\varepsilon_\circ$ is the dielectric constant in vacuum, and *m* is the mass of the electron. When the incident frequency *f* equals f_N, reflection occurs in the ionosphere.

The electron density *N* changes and rises with altitude, reaching a relative maximum and even an absolute maximum electron density N_M, which corresponds to the maximum reflected incidence frequency, called the *critical frequency* f_o (expressed in *MHz*). Thus, for a particular ionospheric layer, f_o is the highest frequency that can be radiated vertically upwards by a radio transmitter and returned to earth [3].

$$N_M = 1.24\ 10^{10}\ f_o^2 \quad (4)$$

The ionospheric layer critical frequency f_o linked to the relative maxima for the *E*- region (f_oE) is referred only to the ordinary ray. The *E* layer f_N is influenced by the solar zenith angle χ and solar activity, which is measured by the monthly median sunspot number *R* according to the empirical equation:

$$f_oE\ (X, R) = 3.3[(1+0.0088R)\cos X]^{1/4}\ MHz \quad (5)$$

It is important to note that the critical frequencies (f_oE), (f_oF1), and (f_oF2), are referred only to the ordinary ray. The virtual height is determined from the time it takes for a radio pulse to travel to and back from a layer in the ionosphere, assuming the pulse travels at the speed of light (*C*). The height of the reflected incident frequency is given by:

$$h' = c\ \Delta t / 2 \quad (6)$$

Where Δt is the delay between the transmission time and the received echo. *h*' is defined as the virtual height or group height.
It has been pointed out that if the virtual height of the layer is known, calculation of the incidence angle needed for the wave to return to the ground at a given point is relatively easy.
The Ionosonde, a vertical ionospheric sounder, emits radio impulses that scan the transmission frequency from 1 to 20 MHz and tests the time delay of any echoes. It is designed to detect electron density of ionospheric plasma as a function of height [12].
The Ionosonde presents an image(Ionogram) that depicts the virtual height of the ionospheric reflection point as a function of frequency, and therefore is a virtual reality instrument (see

Figure 1). The signal is slowed as it passes through the ionosphere, and it is found that the real travel time between the transmitter and receiver is similar to a signal traveling the virtual path, which is not slowed and continues to pass at the speed of light. As a result, the height scale is virtual, and it is much greater than the actual height as the electromagnetic pulse slows and the ionosphere reaches maximum electron density[2].

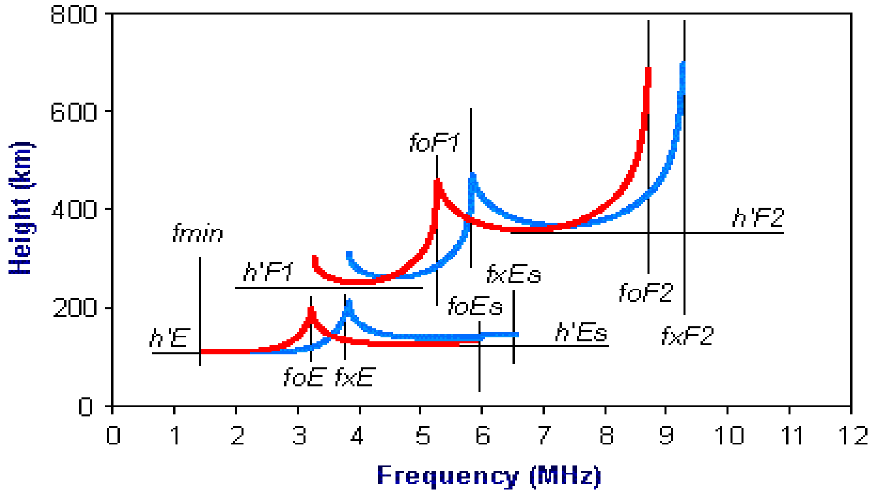

Figure 1: A typical vertical Ionogram. The virtual height is plotted against the receiver frequency[13] .

4. The Solar Activity

Solar radiation is the primary source of ionization in the ionosphere, according to extensive experimental evidence. A long-term cyclical fluctuation is caused by the 11-year sunspot cycle. During this period, the number of sunspots varies from a minimum to a maximum and then back to a minimum [14]. The solar atmosphere experiences an increase in solar flares, filament eruptions, and coronal mass ejections (CMEs) during the ascent phase, resulting in a boost in solar wind energy and an increase in the number of geomagnetic storm events, However, the frequencies of these occurrences decrease during the descent process. The solar activity period has a significant impact on coronal mass ejections, with rates ranging from 0.5 per day at solar minimum to > 6 per day at solar maximum. They are often linked to events like flares, radio bursts, and solar energetic particle events, which can be seen in spectra or images using radio waves, EUV, X rays, and H-alp [15, 16] .

Coronal holes are vast dark areas in the solar atmosphere that can be seen in extreme ultraviolet (EUV) and X-ray imagery. Wide regions of the solar magnetic field with a single polarity (unipolar) and extending far out into the solar system produce these holes. Since these magnetic field lines do not bind back to the Sun, they are often referred to as 'open' magnetic field lines. During the 11-year solar cycle, coronal holes can appear at any time, but they are more common near solar minimum, when recurrent coronal holes can form near the Sun's polar regions. Coronal holes have the potential to expand and migrate to lower solar latitudes [14]. Long-lasting origins of high-speed solar wind streams are persistent coronal holes. A compression area, known as a Co-rotating Interaction Region (CIR), forms as the high-speed stream interacts with the slower ambient solar wind. The CIR would appear to lead the Coronal Hole High-Speed stream(CH HSS) [17]. Strong CIRs and faster CH HSS may have enough of an effect on Earth's magnetosphere to cause G1-G2 (minor to moderate) geomagnetic storming, though rarer cases of stronger storming can also occur. Coronal holes that are wider and vaster can be a source of high solar wind speeds that can last for days [18].
Figure 2 depicts solar cycles and geomagnetic disturbances since 1932. A disturbance has been described as a day on which the Ap index equals or exceeds a value of 25 for the

purposes of this graph, and the number of such days has been counted in each calendar year. In the declining phase of most solar cycles, there is a component that causes large peaks of disturbance. This portion is linked to coronal holes and creates large disturbance peaks during the solar cycles' descending phase.

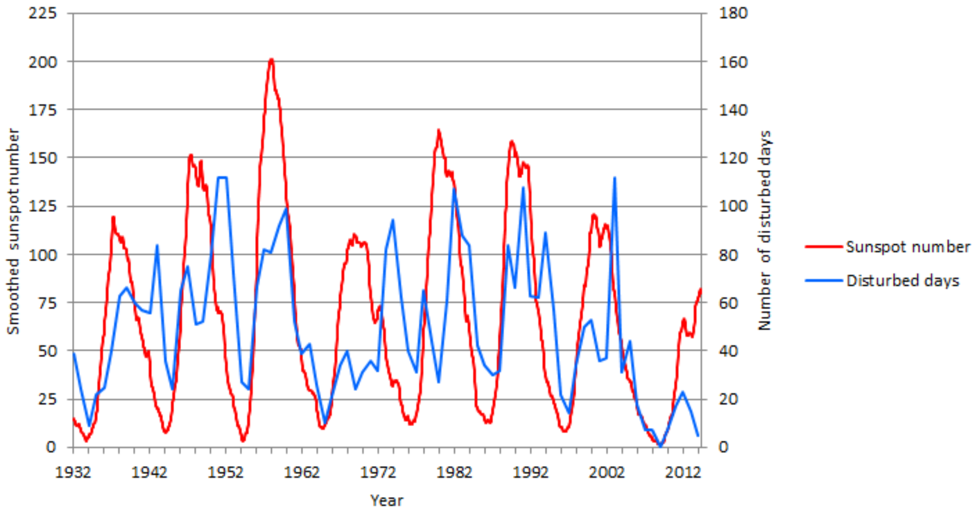

Figure 2: Variation of Sunspot number and the geomagnetic disturbances (1932-2014) [19]

Figure 3 shows the monthly sunspot relative number and the mean smoothed sunspot numbers (the 13-month smoothed) during solar cycle 22 [20]. Cycle 22 which started in September 1986, reached a peak in July 1989 and fell to a minimum in May 1996 [21]. Cycle 22 is still rated as the fourth largest of the recorded cycles [22].

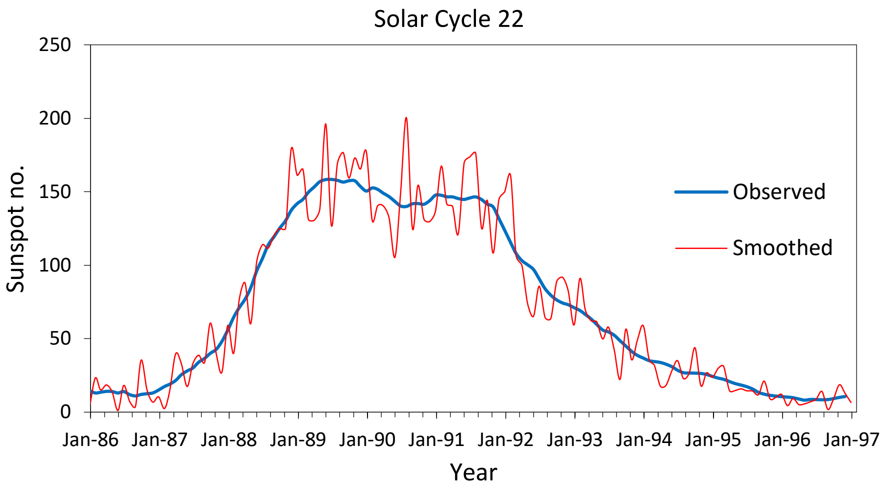

Figure 3: Solar Cycle 22

5. Results and Discussions

The data of the critical frequencies of *E* layer f_oE and the minimum virtual height of the ordinary trace of the *E*- region *h'E* are obtained from Al-Battani Observatory in Baghdad city (latitude 33.3° North, longitude 44.4 ° East). The ionosonde IPS-42 is a vertical ionospheric sounder which emits HF radio impulses that scan the transmission frequency from 1 to 22.6 MHz.

Figure 4(a-k) shows the relation between the monthly mean values of *foE* and diurnal quiet times (in hours) during solar cycle 22(quiet times are durations that not associated with geomagnetic storms). *R* is the monthly mean smoothed sunspot number. For the years 1986 and 1987 there is no available data from the ionosonde. Thus, we began from 1988, until the end of 1995. In addition, there are many discontinuities between 1992 and 1994. Disturbance days, in which magnetic A-index values were greater than or equal to 25, were excluded. Large values of A-index are corresponds to the disturbed condition (major and minor storms). The A indices data were from Fredericksburg Observatory in the USA [23]. These data are generally applicable to mid-latitude areas.

The *foE* values showed high values within the ascent phase of the solar cycle, especially around the maximum at local noon times of Baghdad city. These high values begin to decline gradually, coinciding with the descending phase in which the number of sunspots decrease. At local mid noon times, the mean values of *foE* around the maximum solar activity years (1989, 1990, and 1991) are approximately between (4.2 – 3.4) MHz. These values are drop in 1993, 1994 and 1995, synchronized with the decrease in the sunspot number. The values are limited between (3.5 - 3.1) MHz. However, with increased solar activity, the gap between local mid-afternoon values and dawn and sunset values become wider. It is attributed to the high rate of ionic activity at local noon times during solar maximum years [10, 24, 25].

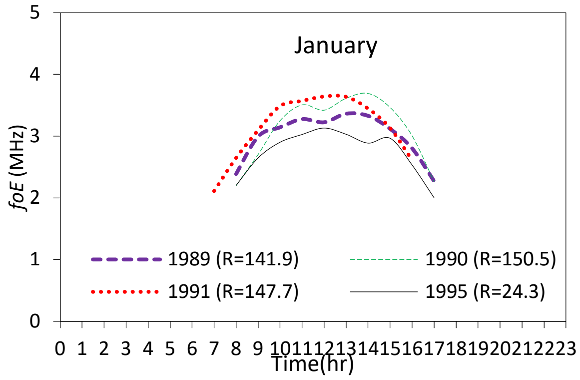

(a)

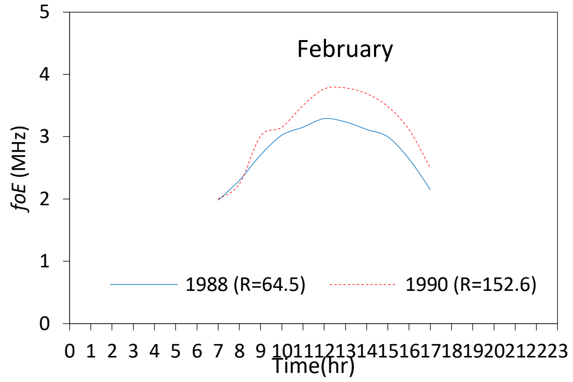

(b)

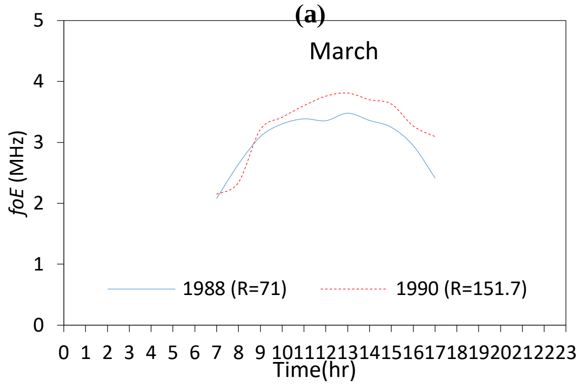

(c)

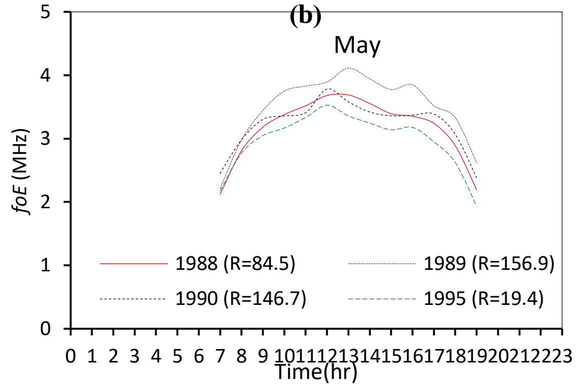

(d)

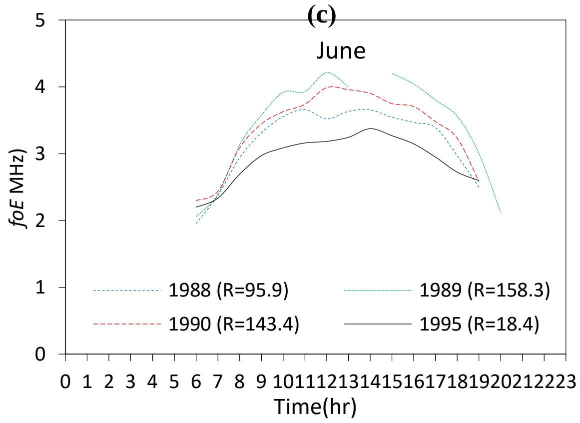

(e)

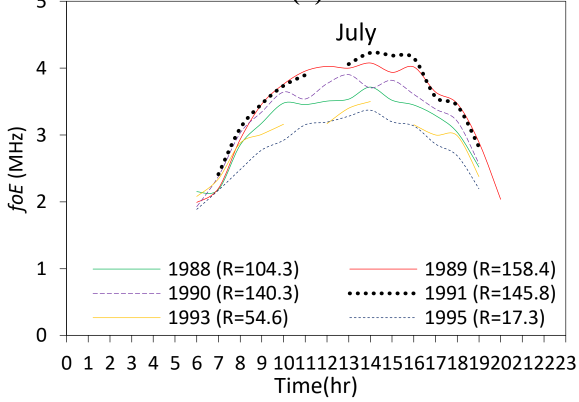

(f)

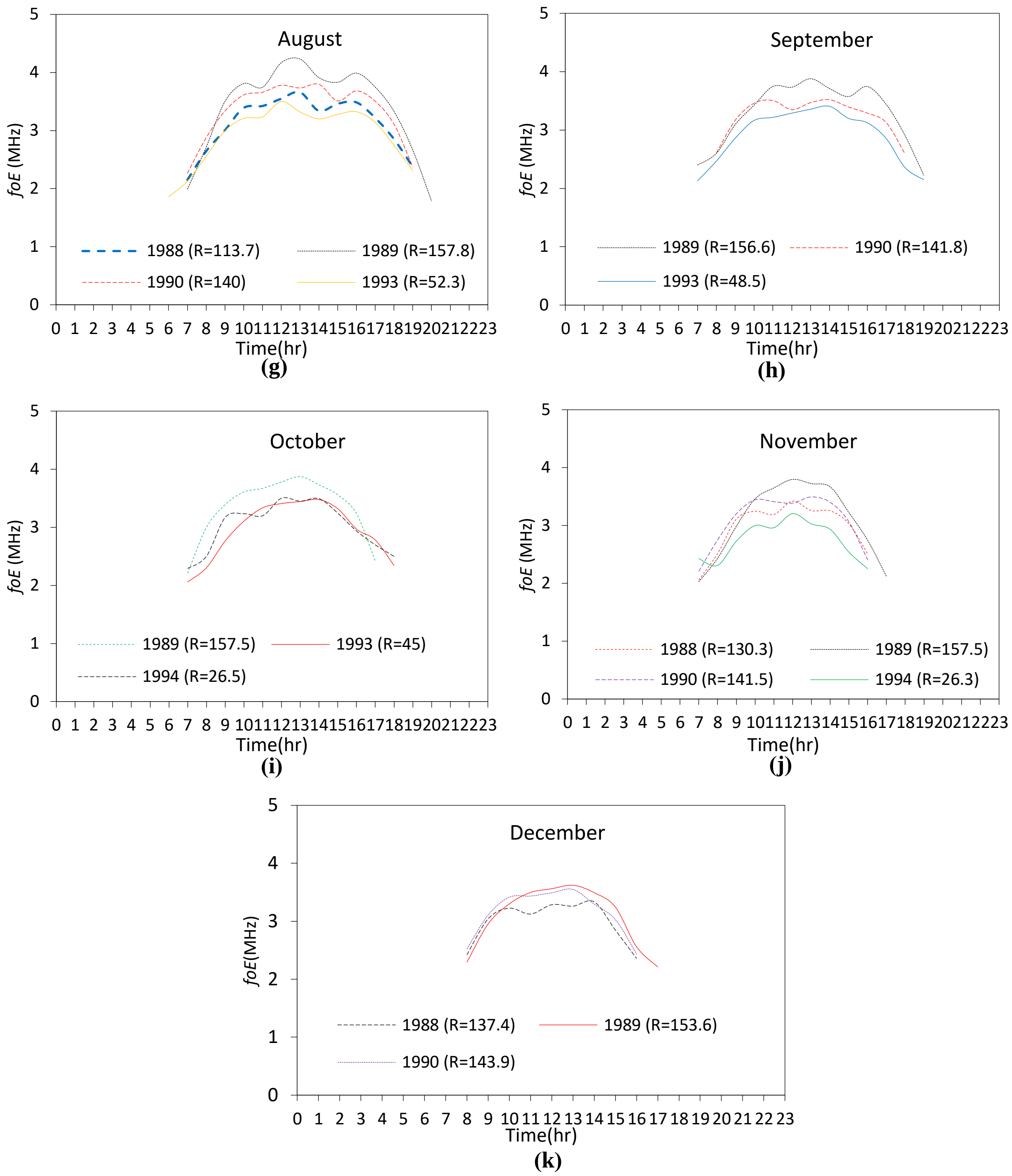

Figure 4 (a-k): The monthly mean values of the critical frequencies of E layer (f_oE)

The high electron-density values of the ionospheric *E* layer could be due to the increased number of active regions on the Sun (sunspots) which cause an increase in EUV emissions with a wavelength of about 17-80 nm. This impacts directly on the electronic concentration of *E* layer (rate of ionization), where most ions are O^+, as well as, the enhancement of the solar particle emission, especially the low energy particles (solar wind) which transfer through interplanetary space, to the magnetosphere, and then to the ionosphere of the earth [1, 10, 11]. During the maximum solar cycle years, the solar atmosphere witnesses an increase in solar flares, filament eruptions and coronal mass ejections CMEs, which leads to a solar wind energy enhancement and a rise in the number of geomagnetic storm events. The occurrence rate of C, M and X class flares was at its maximum between 1989 and 1991, as well as the total solar irradiance(TSI) and the solar 10.7 cm radio flux. (See Figure 5) [26].

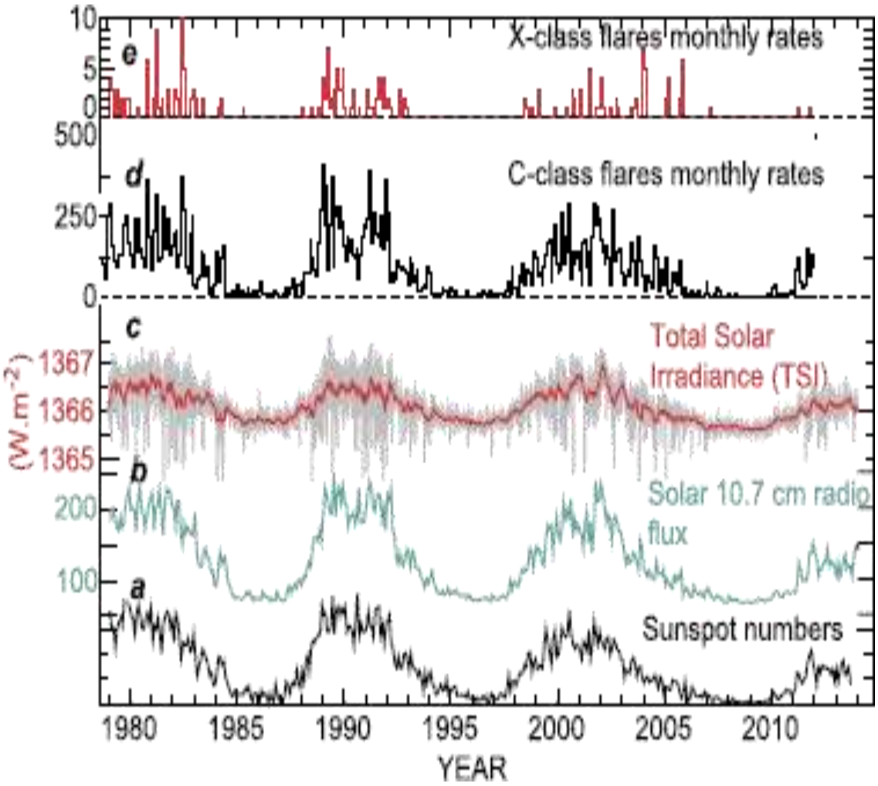

Figure 5: Panels from the bottom display: sunspot numbers, solar 10.7 cm radio flux (W.m^{-2}), TSI, C-class flares monthly rates, and X-class flares monthly rates.

Although the solar cycle descending years witnessed a decline in sunspot number, their critical frequency values are not too far from the ascending phase years. Figure ***6*** displays the variation of the sunspot number and the number of mid-latitude geomagnetic disturbances (major and minor storms) during solar cycle 22. Data archive is available at [27]. For the purposes of this graph, a disturbance has been defined as a day on which the A index ≥ 25.

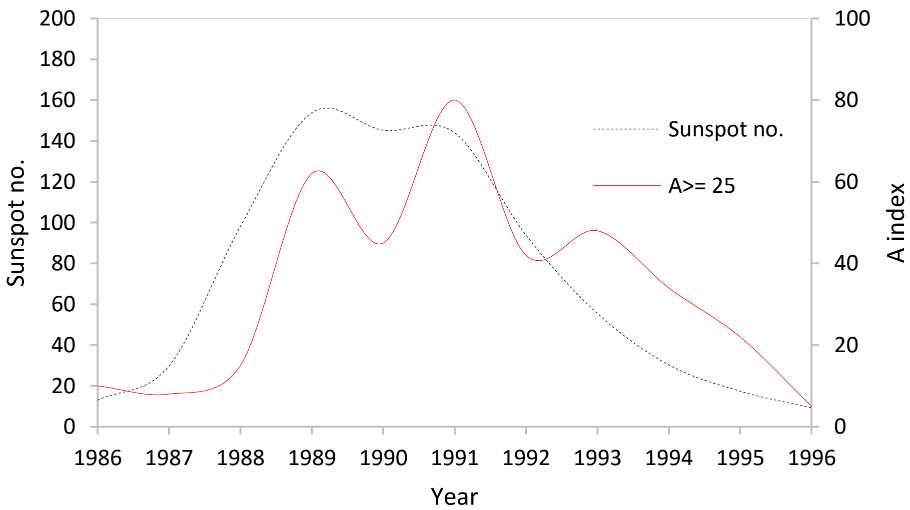

Figure 6: Mid-latitude Magnetic disturbances and Sunspot numbers during Solar cycle 22

Geomagnetic disturbances followes a pattern that is generally identical to the solar cycle, with intervals of decreased disturbance frequency near the solar minimum [28-30].

In the declining phase, there is an aspect indicates to a peak of disturbance. This portion could be linked to coronal holes and resulted in a noticeable increase in the occurance of geomagnetic disturbances between 1992 and 1994. The impact of this portion is obvious in raising the values of foE, especially in 1993.

Figure 7(a-j) shows the relation between the monthly mean values of *h'E* with diurnal monthly quiet times (in hours) during solar cycle 22. At local mid noon times, the mean values of *h'E* around the maximum solar activity years (1989, 1990, and 1991) are approximately between (128.6 – 115) km. These values becomes lower around the minimum years (1993-1995) and sometimes decreases to (102) km. On the other hand, *h'E* values at sunrise reached high altitudes 137 km within maximum solar activity years and 133 km at sunset. However, these values declined sometimes to about 114 km at sunrise and sunset within the minimum years of solar activity.

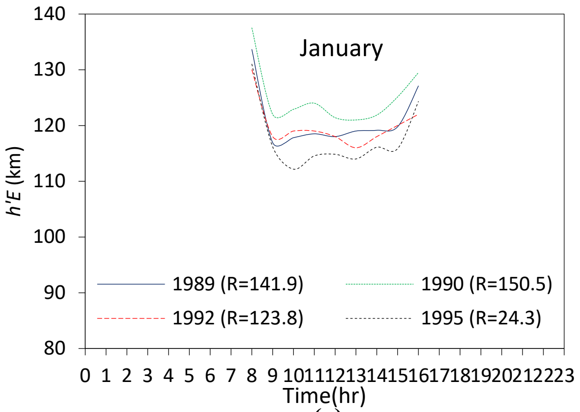

(a)

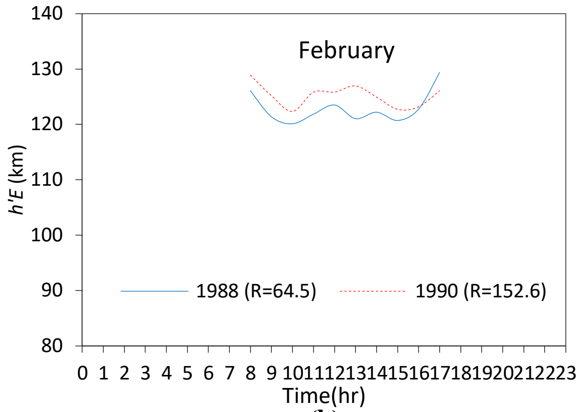

(b)

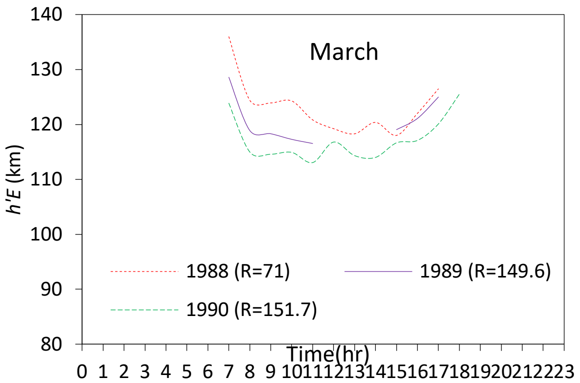

(c)

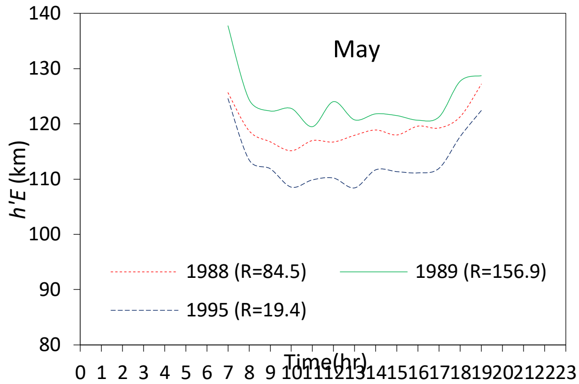

(d)

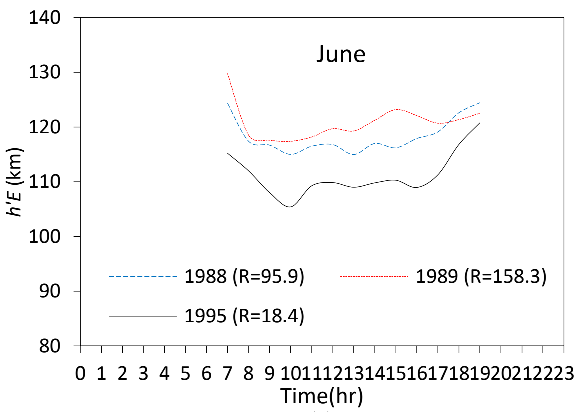

(e)

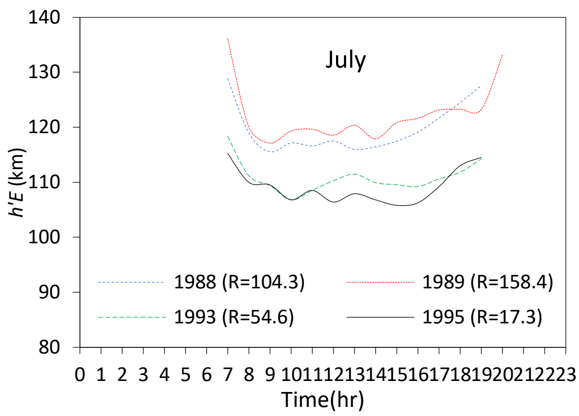

(f)

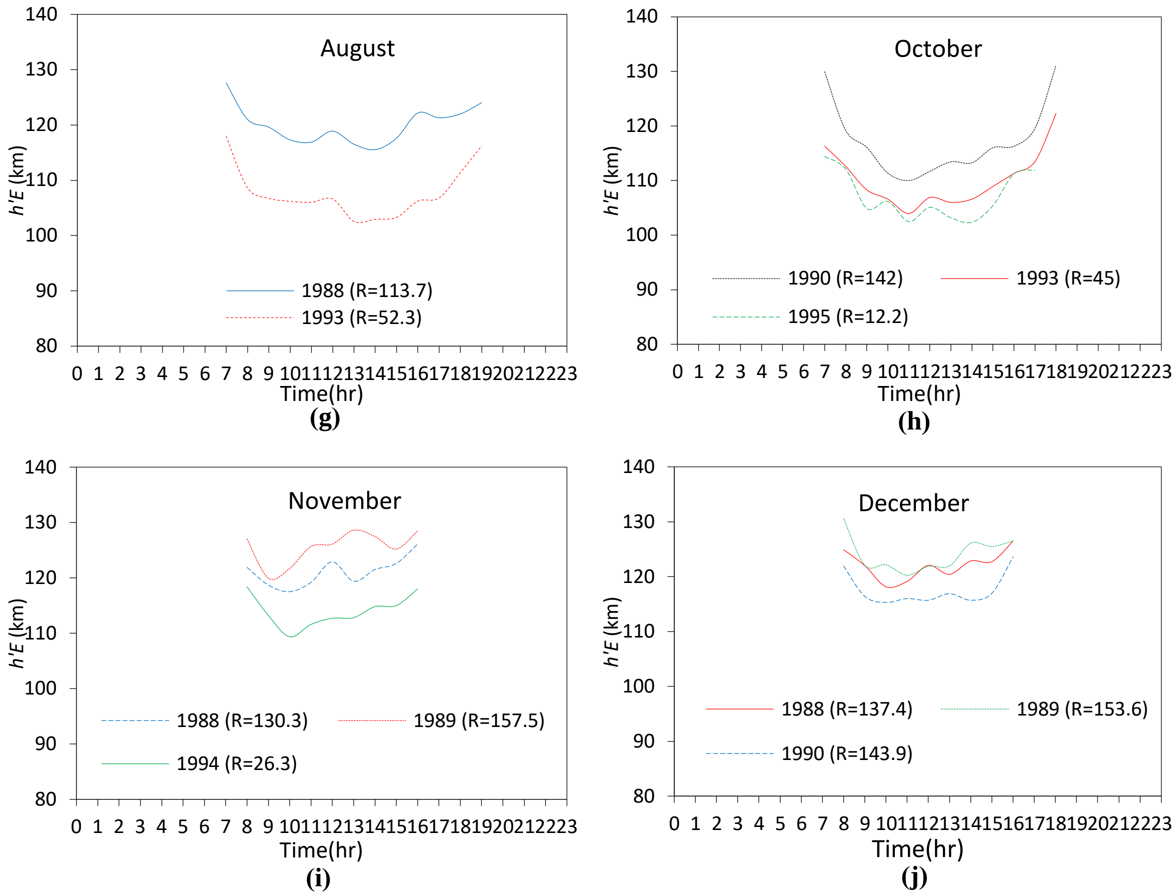

Figure 7(a-j): The monthly mean values of minimum virtual height (*h'E*)

6. Conclusions

Critical frequency and virtual height parameters over Baghdad city showed a high correlation with the sunspot relative numbers within the ascending and descending phases of the solar cycle 22. The *E* layer response to the solar activity is obvious around mid-noon, sunrise and sunset times. furthermore, the gap between local mid-afternoon, dawn and sunset values expands as solar activity increases. In the declining phase, there is an aspect that indicates to a peak of disturbance. This portion could be linked to coronal holes and resulted in a high disturbance peak between 1992-1994. The impact of this portion is obvious in raising the values of f_oE, especially in 1993.

References

[1] H. Rishbeth, "Basic physics of the ionosphere: a tutorial review," *Journal of the institution of Electronic and Radio Engineers*, vol. 58, pp. S207-S223, 1988.

[2] M. C. Kelley, *The Earth's ionosphere: plasma physics and electrodynamics*: Academic press, 2009.

[3] B. Zolesi and L. R. Cander, *Ionospheric prediction and forecasting*: Springer, 2014.

[4] R. A. Ishak, "A study the diurnal and seasonal variation of ionospheric layer above Baghdad and its affected by the solar activity," *Ms.c. thesis, collage of science, Baghdad University*, 1984.

[5] K. Mouala and B. A. Rahman, "Seasonal characteristics of the ionospheric E-region over Baghdad," *Journal of Space and Astronomy Research*, vol. 4, pp. 1-19, 1987.

[6] D. A. AL-Shakarchi, " A study of the solar activity and its effects on the Earth's upper atmosphere," *MSc., Department of Physics, AL-Mustansiriyah University*, 1998.

[7] D. A. Mohammed, M. I. Abdalmajied, and O. T. Ali, "A Study of the Effects of the Solar Cycle 22, on the Critical Frequencies of F1 Layer over Baghdad," *Dirasat, Pure Sciences,* vol. 37, 2010.
[8] K. A. Hadi and A. H. Asma'a, "Investigating the influence of Solar Activity on the Ionospheric Critical Frequencies over Iraqi Region," *Sci Int*, vol. 31, pp. 49-55, 2019.
[9] A. H. Asma'a and K. A. Hadi, "Annual Behavior of Electron Density and Critical Frequency Parameters During Maximum and Minimum Years of Solar Cycles 22, 23 and 24," in *Journal of Physics: Conference Series*, 2021, p. 012065.
[10] K. Davies, *Ionospheric radio*: IET, 1990.
[11] M. P. Hall and L. W. Barclay, "Radiowave-Propagation," *NASA STI/Recon Technical Report A*, vol. 90, p. 45603, 1989.
[12] (2016). *Introduction to HF Radio Propagation*. Available: https://www.sws.bom.gov.au/Educational/5/2/2
[13] B. Brown, Ionogram, Ed., ed: astrosurf.com.
[14] P. V. Foukal, *Solar astrophysics*: John Wiley & Sons, 2008.
[15] N. Gopalswamy, A. Lara, S. Yashiro, S. Nunes, and R. A. Howard, "Coronal mass ejection activity during solar cycle 23," in *Solar Variability as an Input to the Earth's Environment*, 2003, pp. 403-414.
[16] K. Petrovay, "Solar cycle prediction," *Living reviews in solar physics*, vol. 7, pp. 1-93, 2020.
[17] D. A. M. Al-Shakarchi, "A multi-spacecraft study of interacting ICMEs and CIRs in interplanetary space," Aberystwyth University, 2018.
[18] M. J. Owens and R. J. Forsyth, "The heliospheric magnetic field," *Living Reviews in Solar Physics*, vol. 10, pp. 1-52, 2013.
[19] B. o. M. Australian Government, Space Weather Services, Educational, "Magnetic Disturbances and Sunspot Number ", ed: Australian Government, Bureau of Meteorology, Space Weather Services, Educational,, 2014.
[20] SIDC. *Sunspot Bulletin*. Available: http://www.sidc.be/sunspots/bulletins/monthly
[21] J. Alvestad, "Solar Terrestrial Activity Report."
[22] A. S. W. F. Centre. Solar Cycle Number 22 (1986 - 1996) [Online]. Available: https://www.sws.bom.gov.au/Educational/2/3/2
[23] "Geomagnetism," F. O. i. t. USA, Ed., ed: USGS sience for a changing world.
[24] Y. L. Al'pert, "Radio wave propagation and the ionosphere. Volume 1. The ionosphere," 1973.
[25] K. Mouala, "The ionosphere over Iraq and its effects upon HF Radio wave communication (1988- 1990)," *Baghdad, Iraq*, 1991.
[26] A. Balogh, H. Hudson, K. Petrovay, and R. von Steiger, "Introduction to the solar activity cycle: Overview of causes and consequences," *The Solar Activity Cycle*, pp. 1-15, 2015.
[27] "sunspot number and the number of mid-latitude geomagnetic disturbances," ed: Australian Space Weather Forecasting Centre.
[28] W. Gonzalez, B. Tsurutani, and A. C. de Gonzalez, "Geomagnetic storms contrasted during solar maximum and near solar minimum," *Advances in Space Research*, vol. 30, pp. 2301-2304, 2002.
[29] K. Georgieva, "Why the sunspot cycle is double peaked," *International Scholarly Research Notices*, vol. 2011, 2011.
[30] M. J. Owens, M. Lockwood, L. A. Barnard, C. J. Scott, C. Haines, and A. Macneil, "Extreme space-weather events and the solar cycle," *Solar Physics*, vol. 296, pp. 1-19, 2021.